SPE 84369

Multiscale Numerical Modeling of Three-Phase Flow

Ruben Juanes, SPE, Stanford U.; and **Tad W. Patzek**, SPE, U. C. Berkeley / Lawrence Berkeley National Laboratory

This paper was prepared for presentation at the SPE Annual Technical Conference and Exhibition held in Denver, Colorado, U.S.A., 5–8 October 2003.

Abstract

In this paper we present a stabilized finite element method for the numerical solution of three-phase flow in porous media. The key idea of the proposed methodology is a multiscale decomposition into resolved (or grid) scales and unresolved (or subgrid) scales. In the context of subsurface flow and transport, the term multiscale usually refers to subgrid heterogeneity and upscaling. In contrast, this paper deals with unresolved physics: multiple scales are present in the solution even if the medium is homogeneous.

We use the fractional flow approach for the mathematical description of the three-phase flow equations, which leads to a global pressure equation of elliptic type, and a system of conservation laws (the saturation equations). Numerical difficulties in solving these equations include: high nonlinearity, advection-dominated flow, degenerate diffusion, sharpening near-shock solutions, boundary layers, and convergence to nonphysical solutions.

The multiscale formalism allows one to split the original mathematical problem into a grid-scale problem and a subscale problem. The effect of the subgrid scales is then incorporated —in integral form— into the grid-scale equations. Accounting for the subgrid effects results in a finite element method that has enhanced stability properties and is not overly diffusive. Specific original contributions of the methodology proposed herein are: (1) the formulation is applied for the first time to the three-phase flow equations; (2) the fully nonlinear equations in conservation form are used, which is essential for correctly predicting the location of shocks; and (3) a novel expression of a discontinuity-capturing technique is proposed and compared with existing formulations.

The methodology is applied to the simulation of two problems of great practical interest: oil filtration in the vadose zone, and water-gas injection in a hydrocarbon reservoir. These numerical simulations clearly show the potential and applicability of the formulation for solving the highly nonlinear, nearly hyperbolic system of three-phase porous media flow on very coarse grids.

Introduction

Flow of three immiscible fluids —denoted hereafter as water, oil, and gas— occurs in a variety of flow situations in the subsurface, including gas injection into hydrocarbon reservoirs, water flooding in the presence of free gas, and migration of nonaqueous phase liquids in the shallow subsurface. As a result, mathematical and numerical modeling of three-phase flow in porous media has become essential to perform quantitative evaluations and predictions of enhanced oil recovery processes, and environmental remediation of the vadose zone.

In this paper we use a classical mathematical formulation,[1] which is based on a multiphase form of Darcy's equation. By using the fractional flow approach, the mathematical problem of three-phase flow is written as a pressure equation of elliptic type, and a *system* of saturation equations of parabolic type. Because the pressure equation is trivial in the one-dimensional case, we concentrate on the numerical solution of the system of saturation equations.

Even though the equations studied in this paper are a simplified version of the full nonisothermal, multiphase, compositional model in several dimensions, they display some of the essential features that pose numerical difficulties. In particular, the problem is extremely nonlinear, almost hyperbolic for the case of interest —vanishing

capillarity—, and the solution naturally develops shocks and boundary layers. It is well known that, for the type of problems described above, classical numerical methods either lack stability —producing globally oscillatory solutions— or accuracy —solutions are overly diffusive—. In an attempt to obtain stable solutions which retain high-order accuracy, the equations are solved here using a stabilized finite element method.[2] Recently, stabilized finite element methods have been re-interpreted from the point of view of multiscale phenomena,[3] where the stabilizing terms arise naturally in a variational multiscale method.[4] This idea of a multiple-scale decomposition of the solution, which is now dominant in fluid mechanics, is adopted here for the simulation of multiphase, porous media flow. The major benefit of this numerical formulation is that the oscillatory behavior of the classical Galerkin method is drastically reduced. This is achieved without compromising the computational cost of the method, or the accuracy of the solution. The specific contributions of this paper may be succinctly summarized as follows:

1. The multiscale formalism is applied to the equations governing one-dimensional three-phase flow through porous media. Our previous work on miscible and immisicible two-phase flow[5,6] —described by scalar equations— is extended here to nonlinear *systems* of conservation laws.

2. Nonlinearity of the equations is retained at the time of invoking the multiscale split. Proper linearization of the stabilizing terms is introduced *after* the multiple-scale decomposition into resolved and unresolved scales. Furthermore, the multiple-scale solution is *not* reconstructed from point values of coarse and subgrid scales.

3. Several definitions of the key parameter of the formulation —the matrix of stabilizing coefficients— are tested and compared. To further reduce or completely eliminate localized oscillations that may persist in the stabilized solution, several existing shock-capturing techniques are studied, and a novel expression for the discontinuity-capturing diffusion is proposed.

The formulation presented here is quite different from other methods that account for multiple-scale phenomena, such as the multiscale finite element method,[7] the subgrid upscaling technique,[8,9] and the mortar upscaling method,[10] where the main objective is to incorporate the small-scale heterogeneity. In a recent paper,[11] the original variational multiscale formulation[3,4] is applied to the simulation of porous media flows. It is restricted, however, to the linear scalar equation describing steady-state, single-phase, Darcy flow, and the objective is to remove velocity-pressure instabilities, rather than instabilities arising from the nearly hyperbolic character of the equations.

An outline of the paper is as follows. We first present the governing equations of three-phase flow, which are written —in dimensionless form— as a nonlinear system of conservation laws. After a summary of the weak form of the problem and the associated standard Galerkin method, we describe the multiple-scale approach. We then present several representative numerical simulations of three-phase flows. The first application is an oil filtration problem in a relatively dry medium, and the second reproduces water-gas injection in a hydrocarbon reservoir. Numerical solutions are compared with a general, newly developed, analytical solution.[12] These simulations illustrate the performance of the proposed methodology. In the last section, we gather the main conclusions, and anticipate ongoing and future research.

Mathematical formulation

The macroscopic equations governing immiscible multiphase flow in porous media are mass conservation equations and constitutive relations that describe the flux of each phase. Here we study three-phase flow in porous media under the following assumptions:

1. One-dimensional flow,
2. Zero distributed sources and sinks,
3. Immiscible fluids,
4. Incompressible fluids,
5. Rigid homogeneous porous medium,
6. Multiphase flow extension of Darcy's equation,
7. Negligible gravity effects.

When the fractional flow approach is used, the mathematical problem is expressed as a pressure equation of elliptic type, and a system of saturation equations of parabolic type. The solution to the pressure equation is trivial in the one-dimensional case, and we shall concentrate exclusively on the system of saturation equations:

$$\partial_t S_w + v_T \partial_x f_w - \partial_x \left[\frac{k}{\phi} \left(\lambda_w (1 - f_w) \partial_x P_{cw} - \lambda_w f_g \partial_x P_{cg} \right) \right] = 0, \quad (1)$$

$$\partial_t S_g + v_T \partial_x f_g - \partial_x \left[\frac{k}{\phi} \left(-\lambda_g f_w \partial_x P_{cw} + \lambda_g (1 - f_g) \partial_x P_{cg} \right) \right] = 0, \quad (2)$$

where all the quantities are defined in the nomenclature. The derivation of the equations is standard[1,13,14] and will be omitted here.

For a complete definition of the mathematical problem, the functional dependence of the relative permeabilities and capillary pressures needs to be specified. The relative permeabilities are the key descriptors of classical Darcy-type formulations of multiphase flow through porous media. Strictly speaking, relative permeabilities should depend not only on the fluid saturations, but also on the saturation history, wettability characteristics, gravity effects,

and fluid viscosities.[15,16] Thus, they should be properly called *functionals*, rather than functions. In this paper, however, we shall understand the relative permeabilities as functions of fluid saturations alone. In particular, we shall use relative permeabilities that satisfy Stone's assumptions,[17,18] that is, water and gas relative permeabilities depend only on the water and gas saturations, respectively, and oil relative permeability depends on both:

$$\begin{aligned} k_{rw} &= k_{rw}(S_w), \\ k_{ro} &= k_{ro}(S_w, S_g), \\ k_{rg} &= k_{rg}(S_g). \end{aligned} \tag{3}$$

Similar considerations apply to the capillary pressures. In the context of multiphase displacements, capillarity effects lead to a nonlinear diffusion term, whose role is to smear the moving fronts —shocks— that arise in the displacement process. The detailed structure of these shocks —and consequently the capillary pressures—, should depend on several factors, including wettability properties, viscosity ratios, displacement process (drainage or imbibition) and pore-scale fluid configuration.[19] For the purpose of this paper, however, we shall use Leverett's assumption[20,21] that the water and gas capillary pressures depend only on the water and gas saturations, respectively:

$$\begin{aligned} P_{cw} &= P_{cw}(S_w), \\ P_{cg} &= P_{cg}(S_g). \end{aligned} \tag{4}$$

Under these assumptions, the system of saturation equations may be succinctly expressed in *dimensionless form* as follows:

$$\partial_t \boldsymbol{u} + \partial_x \boldsymbol{f} - \partial_x \left(\mathbf{D} \partial_x \boldsymbol{u} \right) = \mathbf{0}, \tag{5}$$

where the independent variables x and t are understood as their dimensionless counterparts, and where

$$\boldsymbol{u} := \begin{pmatrix} S_w \\ S_g \end{pmatrix}, \tag{6}$$

$$\boldsymbol{f} := \begin{pmatrix} f_w \\ f_g \end{pmatrix}, \tag{7}$$

$$\begin{aligned} \mathbf{D} &:= \begin{pmatrix} D_{ww} & D_{wg} \\ D_{gw} & D_{gg} \end{pmatrix} \\ &= \begin{pmatrix} \epsilon_w \lambda_w (1 - f_w) \frac{\mathrm{d}P_{cw}^D}{\mathrm{d}S_w} & -\epsilon_g \lambda_w f_g \frac{\mathrm{d}P_{cg}^D}{\mathrm{d}S_g} \\ -\epsilon_w \lambda_g f_w \frac{\mathrm{d}P_{cw}^D}{\mathrm{d}S_w} & \epsilon_g \lambda_g (1 - f_g) \frac{\mathrm{d}P_{cg}^D}{\mathrm{d}S_g} \end{pmatrix}, \end{aligned} \tag{8}$$

are the vector of unknown saturations, the fractional flow vector and the capillary-diffusion tensor, respectively. The fractional flow vector and the diffusion tensor are (nonlinear) functions of the unknown saturations, *i.e.*,

$$\boldsymbol{f} = \boldsymbol{f}(\boldsymbol{u}), \qquad \mathbf{D} = \mathbf{D}(\boldsymbol{u}). \tag{9}$$

The character of the system (5) depends on the eigenvalues and eigenvectors of the Jacobian matrix $\boldsymbol{f}'$. In previous work,[15,22] we derived conditions on the relative permeability functions so that the eigenvalues of the Jacobian matrix are everywhere real and distinct. Here, we further assume that the capillary diffusion tensor is positive semidefinite. Under these conditions, the system of equations is parabolic, and strictly hyperbolic in the limit of vanishing diffusion.

Multiscale numerical formulation

In this section, we describe a multiscale formulation for the numerical solution of the system (5). We are interested in the case of small diffusion, for which the solution develops sharp features (shocks and boundary layers). The multiscale approach leads naturally to a stabilized numerical method, which enhances the stability of the solution, without compromising its accuracy.

The multiple-scale formalism was first proposed by Hughes,[3] and it is now recognized as a state-of-the-art method in computational fluid dynamics. In our previous work,[5,6] the formulation was applied to miscible flow of two components and immiscible flow of two phases. Here we extend the formulation, and apply it to the problem of three-phase porous media flow.

Initial and boundary value problem The mathematical problem is defined by the one-dimensional system of conservation laws

$$\partial_t \boldsymbol{u} + \partial_x \left(\boldsymbol{f}(\boldsymbol{u}) - \mathbf{D}(\boldsymbol{u}) \partial_x \boldsymbol{u} \right) = \mathbf{0}, \quad x \in \Omega \equiv (0,1), \ t > 0, \tag{10}$$

together with appropriate initial and boundary conditions. We shall consider Dirichlet (essential) and Neumann (natural) boundary conditions. Let $\partial\Omega \equiv \{0,1\}$ be the boundary of the domain, $\Gamma_u \subset \partial\Omega$ is the part of the boundary where essential conditions are imposed, and $\Gamma_n \equiv \partial\Omega \backslash \Gamma_u$ is the part of the boundary with natural boundary conditions:

$$\boldsymbol{u} = \bar{\boldsymbol{u}} \quad \text{on } \Gamma_u, \tag{11}$$

$$(\boldsymbol{f} - \mathbf{D}\partial_x \boldsymbol{u}) n = \bar{\boldsymbol{F}} \quad \text{on } \Gamma_n, \tag{12}$$

where n is the outward unit normal to the boundary, *i.e.*, $n = +1$ at $x = 1$, and $n = -1$ at $x = 0$. The initial conditions

$$\boldsymbol{u}(x, t = 0) = \boldsymbol{u}_0(x), \quad x \in \bar{\Omega} \equiv [0,1], \tag{13}$$

close the definition of the mathematical problem.

Weak form The weak form of the initial and boundary value problem (10)–(13) is obtained by multiplying both sides of the partial differential equation by a suitable test function $\boldsymbol{v}$, integrating over the domain Ω, and integrating by parts the flux term. After these manipulations,[14] the weak form consists in finding, for each fixed t, a smooth-enough function $\boldsymbol{u}$ satisfying the essential boundary condition $\boldsymbol{u} = \bar{\boldsymbol{u}}$ on Γ_u, such that

$$\begin{aligned} 0 = &- \int_{\Gamma_n} \bar{\boldsymbol{F}} \cdot \boldsymbol{v} \, \mathrm{d}\Gamma - \int_\Omega \partial_t \boldsymbol{u} \cdot \boldsymbol{v} \, \mathrm{d}\Omega \\ &+ \int_\Omega \boldsymbol{f}(\boldsymbol{u}) \cdot \partial_x \boldsymbol{v} \, \mathrm{d}\Omega - \int_\Omega \mathbf{D}(\boldsymbol{u}) \partial_x \boldsymbol{u} \cdot \partial_x \boldsymbol{v} \, \mathrm{d}\Omega \end{aligned} \tag{14}$$

for all smooth-enough test functions $\boldsymbol{v}$ with $\boldsymbol{v} = \boldsymbol{0}$ on Γ_u. Equation (14) is linear in the test function $\boldsymbol{v}$. This fact is exploited at the implementation level, for it allows to consider test functions of the form:

$$\boldsymbol{v} = \begin{pmatrix} v_1 \\ 0 \end{pmatrix} + \begin{pmatrix} 0 \\ v_2 \end{pmatrix}. \tag{15}$$

The problem is infinite-dimensional, in the sense that the sets of trial functions $\boldsymbol{u}$ and test functions $\boldsymbol{v}$ are infinite.

Classical Galerkin method Once the mathematical problem has been stated in weak form, it is straightforward to introduce the classical Galerkin method. Rather than considering infinite-dimensional spaces of trial and test functions, only finite sets are employed. Given a partition of the domain Ω into non-overlapping elements, the trial and test functions are restricted to be linear combinations of the usual *finite element basis functions* (conforming piecewise polynomials with local support). In the Galerkin method, the same basis functions are used to define the trial functions $\boldsymbol{u}_h$ and the test functions $\boldsymbol{v}_h$. The standard Galerkin approximation reduces to find the finite element function $\boldsymbol{u}_h$ satisfying $\boldsymbol{u}_h = \bar{\boldsymbol{u}}$ on Γ_u, such that:

$$\begin{aligned} 0 = &- \int_{\Gamma_n} \bar{\boldsymbol{F}} \cdot \boldsymbol{v}_h \,\mathrm{d}\Gamma - \int_\Omega \partial_t \boldsymbol{u}_h \cdot \boldsymbol{v}_h \,\mathrm{d}\Omega \\ &+ \int_\Omega \boldsymbol{f}(\boldsymbol{u}_h) \cdot \partial_x \boldsymbol{v}_h \,\mathrm{d}\Omega - \int_\Omega \mathbf{D}(\boldsymbol{u}_h) \partial_x \boldsymbol{u}_h \cdot \partial_x \boldsymbol{v}_h \,\mathrm{d}\Omega \end{aligned} \tag{16}$$

for all finite element test functions $\boldsymbol{v}_h$ with $\boldsymbol{v}_h = \boldsymbol{0}$ on Γ_u. The system of ordinary differential equations (16) is transformed into a system of (nonlinear) algebraic equations by further discretizing the time derivative.

Multiple-scale approach It is well-known that the classical Galerkin method lacks stability when diffusive effects are exceedingly small, so that the system of equations is nearly hyperbolic. The objective of the multiple-scale approach described here is to obtain a stabilized numerical formulation for this type of problems. The key idea of the formulation is a multiscale split of the variable of interest $\boldsymbol{u}$ into resolved and unresolved scales:

$$\boldsymbol{u} = \boldsymbol{u}_h + \tilde{\boldsymbol{u}}, \tag{17}$$

where $\boldsymbol{u}_h$ is the resolved —grid— scale and $\tilde{\boldsymbol{u}}$ is the unresolved —subgrid— scale. This decomposition acknowledges that certain components of the solution cannot be captured by the finite element mesh. This fact is especially relevant for advection-dominated problems, where the solution develops sharp features that would require an impractical grid resolution.

The derivation of the multiscale formulation starts by invoking a multiscale split of the solution $\boldsymbol{u}$ and the test function $\boldsymbol{v}$:

$$\boldsymbol{u} = \boldsymbol{u}_h + \tilde{\boldsymbol{u}}, \tag{18}$$

$$\boldsymbol{v} = \boldsymbol{v}_h + \tilde{\boldsymbol{v}}. \tag{19}$$

Because the weak form is linear with respect to the test function $\boldsymbol{v}$, the original mathematical problem (14) is split into two: a grid scale problem and a subscale problem.[14]The former is a finite-dimensional problem, whereas the latter is infinite-dimensional.

The *subscale problem* is modeled, rather than solved, by an algebraic subgrid scale (ASGS) approximation:

$$\tilde{\boldsymbol{u}} \approx \boldsymbol{\tau}_{u_h} \mathcal{R}(\boldsymbol{u}_h), \tag{20}$$

where $\mathcal{R}(\boldsymbol{u}_h)$ is the grid scale residual:

$$\mathcal{R}(\boldsymbol{u}_h) := -\partial_t \boldsymbol{u}_h - \partial_x \big(\boldsymbol{f}(\boldsymbol{u}_h) - \mathbf{D}(\boldsymbol{u}_h) \partial_x \boldsymbol{u}_h \big), \tag{21}$$

and where $\boldsymbol{\tau}_{u_h}$ is a 2×2 matrix of algebraic coefficients, which depend not only on the system parameters, but also on the grid scale solution $\boldsymbol{u}_h$. This approximation is substantiated by the convergence analysis of the linear case.[23] It can also be justified from an asymptotic Fourier analysis,[23] and has proven useful in numerical tests. The matrix $\boldsymbol{\tau}_{u_h}$ is known as the matrix of stabilizing coefficients or matrix of intrinsic time scales,[24] and has dimensions of time. Its design, which should be ultimately dictated by stability and convergence analysis, is one of the most difficult issues in the development of a stabilized numerical method. Many alternatives have been proposed, some of which are reviewed and succinctly described below.

After several manipulations and assumptions,[14] the *grid scale equation* takes the following form:

$$\begin{aligned} 0 = &- \int_{\Gamma_n} \bar{\boldsymbol{F}} \cdot \boldsymbol{v}_h \,\mathrm{d}\Gamma - \int_\Omega \partial_t \boldsymbol{u}_h \cdot \boldsymbol{v}_h \,\mathrm{d}\Omega \\ &+ \int_\Omega \boldsymbol{f}(\boldsymbol{u}_h) \cdot \partial_x \boldsymbol{v}_h \,\mathrm{d}\Omega - \int_\Omega \mathbf{D}(\boldsymbol{u}_h) \partial_x \boldsymbol{u}_h \cdot \partial_x \boldsymbol{v}_h \,\mathrm{d}\Omega \\ &- \sum_e \int_{\Omega^e} \mathcal{L}^*_{u_h} \boldsymbol{v}_h \cdot \tilde{\boldsymbol{u}} \,\mathrm{d}\Omega, \end{aligned} \tag{22}$$

The differential operator $\mathcal{L}^*_{u_h}$ is the adjoint of a linearized advection-diffusion operator:

$$\mathcal{L}^*_{u_h} \boldsymbol{v} := -\mathbf{A}^T(\boldsymbol{u}_h) \partial_x \boldsymbol{v} - \partial_x (\mathbf{D}^T(\boldsymbol{u}_h) \partial_x \boldsymbol{v}), \tag{23}$$

where

$$A_{ij}(\boldsymbol{u}_h) := \frac{\partial f_i(\boldsymbol{u}_h)}{\partial u_{h,j}} - \sum_k \frac{\partial D_{ik}(\boldsymbol{u}_h)}{\partial u_{h,j}} \partial_x u_{h,k}. \tag{24}$$

By direct comparison with Eq. (16), it is immediate to identify in Eq. (22) the Galerkin terms and the additional stabilizing term of the multiscale formulation. The grid scale equation and the subgrid scale equation are coupled through the value of the subscales $\tilde{\boldsymbol{u}}$. For the simple subgrid scale model employed here, the algebraic approximation (20) is substituted in Eq. (22). An important property of the variational multiscale method is that, because the subscales are proportional to the grid-scale residual, the formulation is residual-based and, therefore, automatically consistent.

The novel features of our formulation are:[14]

1. Linearization of the equations is employed *after* the multiscale split. In particular, only the subscale effects are linearized, whereas the full nonlinear Galerkin term is retained in the grid scale equation.

2. The approximate solution is *not* reconstructed from point values of the coarse-scale and subgrid-scale solutions. The subscales enter the coarse-scale problem in integral form.

Matrix of stabilizing coefficients The design of the matrix of intrinsic time scales $\boldsymbol{\tau}_{u_h}$ is one of the most difficult —and controversial— issues in the development of a stabilized formulation. In this paper we consider several alternatives.

Definition through an eigenvalue problem The matrix of stabilizing coefficients, based on the form proposed by Hughes and Mallet,[24] is given by:

$$\boldsymbol{\tau}_{u_h} = \mathbf{R}\hat{\boldsymbol{\tau}}_{u_h}\mathbf{R}^T, \tag{25}$$

where $\mathbf{R} = [\boldsymbol{r}_1, \ldots, \boldsymbol{r}_n]$. We denote by ν_i, $\boldsymbol{r}_i$, the eigenvalues and eigenvectors of the advection matrix $\mathbf{A}$, and

$$\hat{\boldsymbol{\tau}}_{u_h} = \mathrm{diag}(\hat{\tau}_1, \ldots, \hat{\tau}_n), \tag{26}$$

where

$$\hat{\tau}_i = \frac{1}{2}h\frac{\hat{\xi}(\alpha_i)}{|\nu_i|}, \qquad \hat{\xi}(\alpha_i) = \coth(\alpha_i) - \frac{1}{\alpha_i},$$
$$\alpha_i = \frac{1}{2}\frac{|\nu_i|h}{\epsilon_i}, \qquad \epsilon_i = \boldsymbol{r}_i^T\mathbf{D}\boldsymbol{r}_i.$$

Since the advection and diffusion matrices change from point to point, an eigenvalue problem needs to be solved at each integration point.

Definition through the matrix inverse A different design of the matrix of intrinsic time scales was proposed by Codina[25] based on an analysis of the discrete maximum principle:

$$\boldsymbol{\tau}_{u_h} = \left(\frac{c_1}{h^2}\mathbf{D}(\boldsymbol{u}_h) + \frac{c_2}{h}\mathbf{A}(\boldsymbol{u}_h)\right)^{-1}, \tag{27}$$

where $c_1 = 4$ and $c_2 = 2$ for linear finite elements.

Shock-capturing techniques To enhance the robustness of the stabilized formulation, we incorporate a discontinuity-capturing term. It takes the form of an extra diffusion term, where the numerical diffusion D_{sc} depends on the coarse scale solution. The "canonical" form[26] is:

$$D_{sc,1} = \frac{1}{2}h\frac{|\mathcal{R}(\boldsymbol{u}_h)|}{|\partial_x\boldsymbol{u}_h|}. \tag{28}$$

We propose a different expression, where the local gradient $\partial_x\boldsymbol{u}_h$ is replaced by a global measure of the gradient $\sim \boldsymbol{U}_{sc}/h$:

$$D_{sc,g} = C_{sc}h\frac{|\mathcal{R}(\boldsymbol{u}_h)|}{|\boldsymbol{U}_{sc}/h|}, \tag{29}$$

where C_{sc} is a constant coefficient. The simulations of the next section show that this formulation introduces numerical diffusion in narrower regions of the computational domain than the classical formulation.

Numerical simulations

In this section we present several simulations of one-dimensional three-phase flow in porous media, as described by the mathematical model of the previous sections. For the sole purpose of testing the formulation, the capillary diffusion tensor is taken as a constant isotropic matrix, that is, Eq. (8) is replaced by:

$$\mathbf{D} = \begin{pmatrix} \epsilon_w & 0 \\ 0 & \epsilon_g \end{pmatrix}. \tag{30}$$

The *form* of the capillary diffusion tensor may affect the detailed structure of individual shocks, but not the shock location and the global structure of the solution. The practical importance of this dependency on the form of the diffusion tensor is minimized by the fact that, because we are interested in the nearly hyperbolic case —which is the most challenging to model numerically—, we shall use very small values of the capillary diffusion coefficients ϵ_w, ϵ_g.

The following relative permeability functions are used:

$$\begin{aligned} k_{rw} &= S_w^2, \\ k_{ro} &= (1-S_w)(1-S_g)(1-S_w-S_g), \\ k_{rg} &= \beta_g S_g + (1-\beta_g)S_g^2. \end{aligned} \tag{31}$$

These functions belong to the simple class of functions (3), where the water and gas relative permeabilities depend only on their own saturation, and the oil relative permeability depends on both. The parameter β_g is the endpoint-slope of the gas relative permeability function. The relevance of this parameter in the context of classical relative permeability models is discussed elsewhere.[15,27] In the simulations that follow we use the value $\beta_g = 0.1$. Finally, the following values of the fluid viscosity ratios are used:

$$\frac{\mu_w}{\mu_o} = 0.4375, \quad \frac{\mu_g}{\mu_o} = 0.015. \tag{32}$$

The simulations presented here reproduce the conditions of the *Riemann problem*, which is an initial value problem on an unbounded domain defined by the system of conservation laws (10), together with piecewise constant initial data separated by a single discontinuity:

$$\boldsymbol{u}(x,0) = \begin{cases} \boldsymbol{u}_l & \text{if } x < 0, \\ \boldsymbol{u}_r & \text{if } x > 0. \end{cases} \tag{33}$$

We model conditions (33) numerically by imposing the initial condition $\boldsymbol{u}(x,0) = \boldsymbol{u}_r$ on a *bounded* domain $0 < x < 1$, and a Dirichlet boundary condition $\boldsymbol{u}(0,t) = \boldsymbol{u}_l$ on the left boundary. The interest in the Riemann problem is threefold. On one hand, it is particularly challenging to model numerically, since the initial conditions are already

discontinuous. Secondly, an analytical solution exists for the capillarity-free case, which can be used to verify the numerical solutions.[12,22] Finally, it is very valuable in practical applications, because many laboratory and field experiments reproduce approximately the conditions of the Riemann problem.

Here we study two scenarios: the first one involving oil filtration in a relatively dry soil, and the second one reproducing water-gas injection in an oil reservoir. Both simulations are transient over a period of time —the solution displays propagating discontinuities—, and then reach quasi-steady conditions —boundary layers are present at the outlet face—. For each of the two problems studied, we compare the exact solution of the capillarity-free model with the numerical solution obtained using the standard Galerkin method on a very fine mesh. Then we compare the performance —on a very coarse mesh— of the classical Galerkin method with the algebraic subgrid scale method, using different formulations for the matrix of stabilizing coefficients. Different discontinuity-capturing formulations are also employed and contrasted. The comparison of stabilized formulations with the standard Galerkin method may seem a little unfair, as the test cases involve nearly hyperbolic systems, for which the classical Galerkin method is known to have unstable behavior. The motivation is to show the stabilizing effect of the new terms in the ASGS formulation, which arise from consideration of the subgrid scales. It is interesting to note that:

1. The ASGS method is in fact a Galerkin method, because the coarse-scale trial and test functions belong to the same finite element space. The difference with respect to the classical Galerkin method is that the subgrid scales are modeled separately and incorporated into the coarse scale problem.

2. The computational cost of the ASGS method is essentially the same as that of the standard Galerkin method, as the former involves the calculation of just a few additional integrals, which are evaluated elementwise.

Oil filtration in relatively dry soil This example reproduces filtration of a mixture of oil, water and gas through a relatively dry porous medium with some water and oil, as shown in **Fig. 1**. The medium has the following initial normalized saturations: $S_w = 0.15$, $S_g = 0.8$, and $S_o = 0.05$. Fluids are injected in a proportion such that the normalized fluid saturations at the inlet face are: $S_w = 0.25$, $S_g = 0.2$, and $S_o = 0.55$. Initial saturations are homogeneous on the entire medium, and injected saturations are held constant throughout the experiment, so that the example reproduces the conditions of the Riemann problem. From a practical viewpoint, this problem could represent a contamination event in the shallow subsurface, under one-dimensional flow conditions.

Analytical solution In this case, the exact solution to the strictly hyperbolic system of the capillarity-free problem consists in a sequence of two genuine shocks.[12] The solution is shown in saturation space in **Fig. 2**. It is important to note that dashed lines correspond to the shock curves, and represent discontinuities in the solution. Therefore, the actual path of the shock curves on the saturation triangle is inconsequential from the point of view of the saturation profiles, and what matters is the location of the endpoints of each shock curve.

In **Fig. 3** we display in a single plot the profiles of water, gas, and oil saturations against the similarity variable $\zeta = x/t$. The solution at different times can be obtained from one another by simple stretching. The saturations at the right boundary coincide with the initial state, and the saturations at the left boundary correspond to the injected state. This figure clearly illustrates the behavior of the displacement process: basically, the oil phase displaces the water phase, which in turn displaces gas out of the porous medium. One of the key features of the solution is the formation of a water bank —a region where the water saturation is higher than that of the initial and injected states—, so that the solution is *not* monotonic in the traditional sense. It is also interesting to note that the slow shock involves changes in all three saturations, whereas the fast shock connects states with approximately the same oil saturation (see also Figure 2).

"Reference" numerical solution We test whether the numerical solution to the three-phase oil filtration problem *with capillarity* provides an accurate approximation to the analytical solution of the capillarity-free case above. Since we are interested in the nearly hyperbolic case, we take small values of the capillary diffusion coefficients in Eq. (30):

$$\epsilon_w = 0.0005, \quad \epsilon_g = 0.001. \tag{34}$$

We compute a "reference" numerical solution using the standard Galerkin method on a very fine mesh of 4000 elements. We use a Crank-Nicolson time integration technique with a constant time step of $\delta t = 10^{-4}$. Given this discretization and the physical parameters of the problem —in particular the speed of propagation $\sigma_{\max}$ of the fast shock—, we may define the following dimensionless parameters:

$$Pe := \frac{\sigma_{\max}\, h}{\epsilon_{\min}} \approx 0.1 \qquad \text{(element Peclet number)}, \tag{35}$$

$$Co := \frac{\sigma_{\max}\, \delta t}{h} \approx 0.08 \quad \text{(element Courant number)}. \tag{36}$$

The space and time discretization have been chosen to obtain small values of these two key parameters ($Pe \ll 1$, $Co \ll 1$), so that the reference solution given by the classical Galerkin method is stable and accurate. The comparison between this solution and the analytical solution described above is presented in **Fig. 4** at time $t = 3$. The "reference" numerical solution captures correctly the global structure of the capillarity-free solution: the location of shocks and the magnitude of the intermediate constant state are predicted accurately. Further numerical

Fig. 1— Sketch of the oil filtration problem. A mixture with high oil saturation is injected into a relatively dry medium.

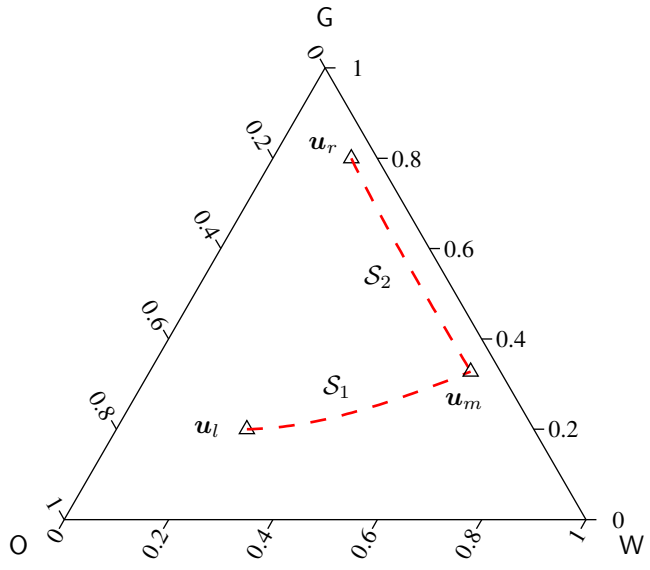

Fig. 2— Saturation path of the exact solution to the oil filtration problem. Both waves are genuine shocks.

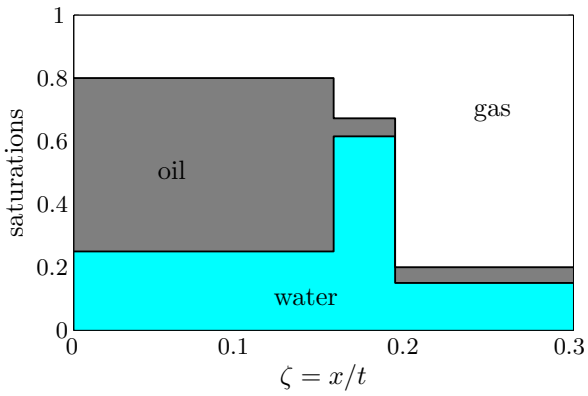

Fig. 3— Saturation profiles of the exact solution to the oil filtration problem. Saturations of each phase are plotted against the similarity variable $\zeta = x/t$.

simulations —using different values of the capillary diffusion coefficients and different number of elements— confirm that the standard Galerkin solution converges to the entropy solution of the capillarity-free problem.

Standard Galerkin solution The same problem is solved using the standard Galerkin method on a coarse mesh of only 40 elements. The element Peclet number is now $Pe \approx 10$. A Crank-Nicolson time-stepping with $\delta t = 0.01$ is used. The associated Courant number is still very small ($Co \approx 0.08$), to minimize the numerical error introduced by the time discretization. The results of this simulation are shown in **Fig. 5**. The solution obtained with the classical Galerkin method on a fine mesh of 4000 elements is included for reference. Water and gas saturation profiles are plotted at two different times: $t = 3$ (transient conditions), and $t = 8$ (quasi-steady conditions). It is apparent that the standard Galerkin solution on a coarse grid lacks stability, and is polluted with spurious oscillations. The instabilities are especially severe for the long-term solution, where the oscillatory behavior spreads over most of the computational domain.

Algebraic subgrid scale solutions We present now the numerical solution to the oil filtration problem obtained with the algebraic subgrid scale (ASGS) method. We recall that the ASGS formulation —Eq. (22)— differs from the classical Galerkin method —Eq. (16)— in the addition of a stabilizing term, evaluated element by element. This stabilizing term involves the subgrid scales, which are modeled analytically using an algebraic approximation to the subscales —Eq. (20)—. Different alternatives for the definition of the matrix $\boldsymbol{\tau}$ of stabilizing coefficients were discussed above.

In **Fig. 6** we plot the results obtained with the ASGS method and the definition of $\boldsymbol{\tau}$ given by the eigenvalue problem (25) (formulation proposed by Hughes and Mallet[24]). The solution is much stabler than the standard Galerkin solution. The computed saturation profiles do not display global oscillatory behavior, and capture sharply the transient shocks and the stationary boundary layers. Some small overshoots and undershoots remain, however, but they are confined to the vicinity of the sharp features in the solution.

The ASGS solution obtained with the $\boldsymbol{\tau}$ matrix given by the matrix inverse (27) (formulation proposed by Codina[25]) is shown in **Fig. 7**. The solution is virtually identical to that of Figure 6, and the same comments apply.

Stabilized solutions with shock capturing diffusion In an attempt to reduce, or completely eliminate, the localized wiggles that remain in the solution of the stabi-

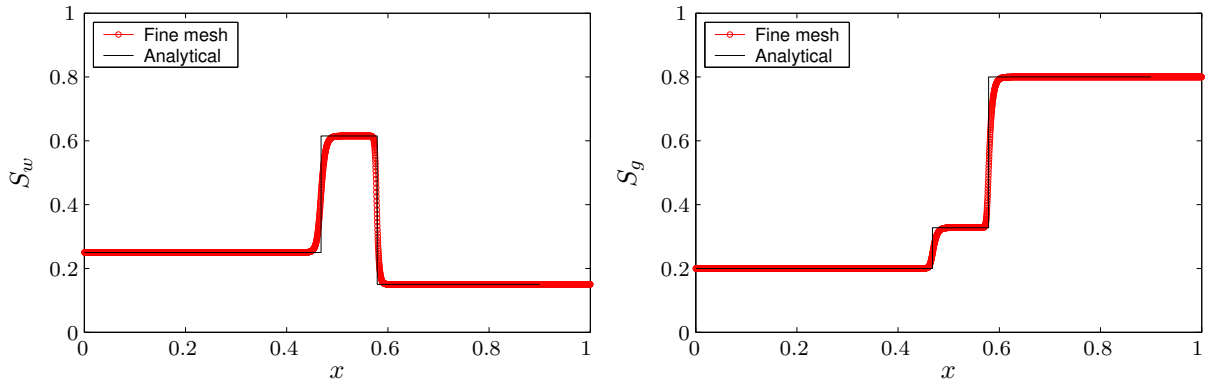

(a) Water saturation (b) Gas saturation

Fig. 4— Saturation profiles of the standard Galerkin solution to the oil filtration problem on a fine mesh of 4000 elements, and comparison to the analytical solution of the capillarity-free case. Results are shown at time $t = 3$.

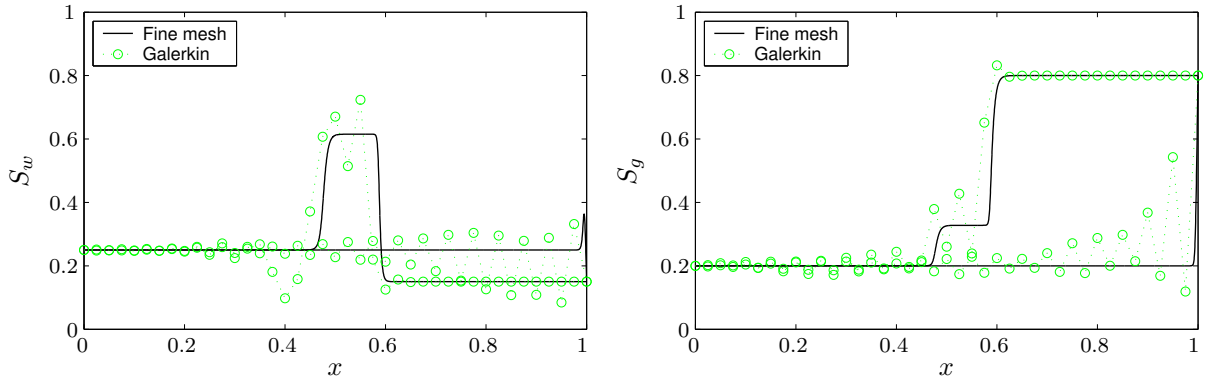

(a) Water saturation (b) Gas saturation

Fig. 5— Saturation profiles of the standard Galerkin solution to the oil filtration problem on a coarse mesh of 40 elements. Results are shown at times $t = 3$ and $t = 8$.

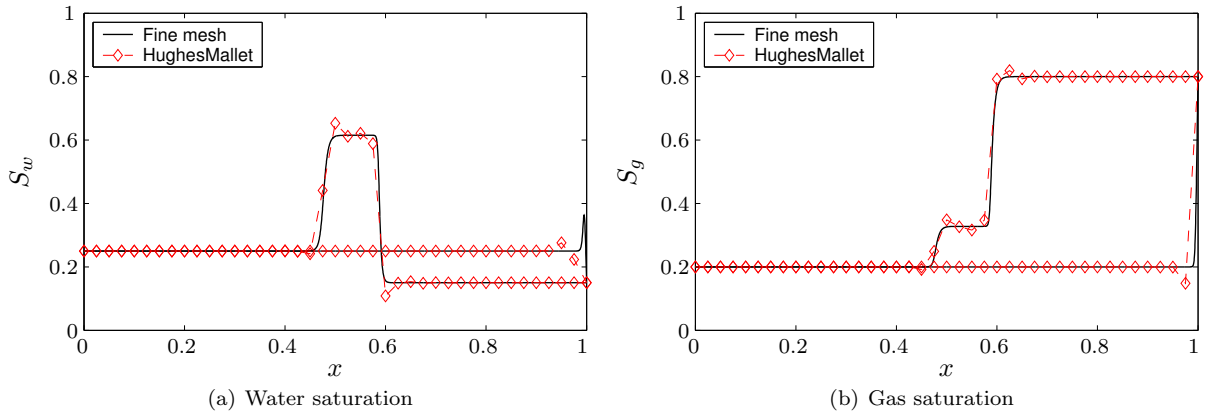

(a) Water saturation (b) Gas saturation

Fig. 6— Saturation profiles of the ASGS solution (τ formulation given by Hughes and Mallet[24]) to the oil filtration problem on the coarse mesh.

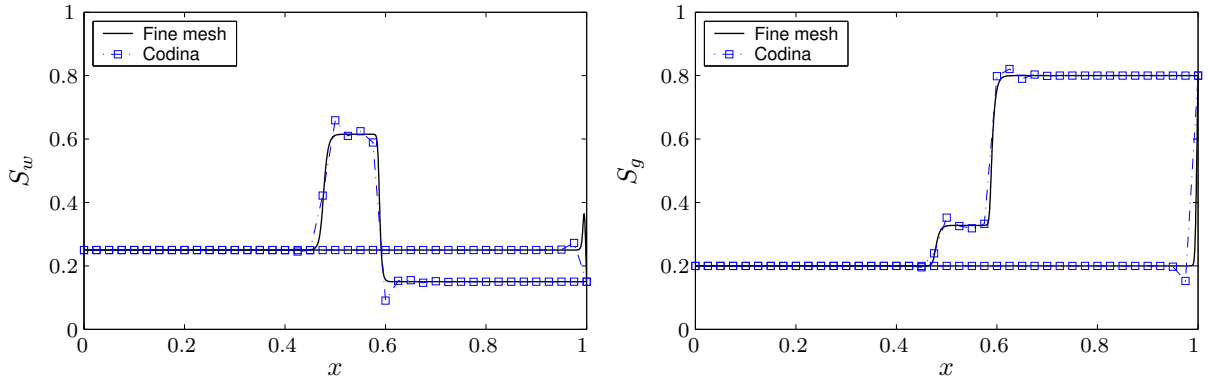

(a) Water saturation (b) Gas saturation

Fig. 7— Saturation profiles of the ASGS solution (τ formulation given by Codina[25]) to the oil filtration problem on the coarse mesh.

lized ASGS method —Figures 6 and 7 above—, we test several shock-capturing techniques. We compare different expressions of the discontinuity-capturing diffusion applied to the same ASGS method. In this case, we choose the solution obtained with the $\boldsymbol{\tau}$ matrix of Hughes and Mallet[24] —Figure 6—.

In **Fig. 8** we plot the results for the "canonical form" of the shock-capturing diffusion —Eq. (28)—. It is found that this formulation is effective at eliminating the oscillatory behavior (compare with Figure 6), but at the cost of being a bit too diffusive.

In **Fig. 9** we plot the numerical solution obtained when the novel "global-gradient form" of the discontinuity-capturing diffusion is employed —Eq. (29)—, with the following values of the parameters:

$$\boldsymbol{U}_{sc} = (0.5, 0.5), \qquad C_{sc} = 2. \tag{37}$$

The method is able to remove the localized oscillatory behavior of the ASGS solution but is, for the parameters used, slightly too diffusive as well.

The reason for considering the novel expression of the shock-capturing diffusion as a viable alternative to existing formulations stems from the behavior of the numerical diffusion that is actually introduced by each method. In **Fig. 10** and **Fig. 11** we plot the profile of additional diffusion introduced by the "canonical form" and the "global-gradient form", respectively, at two different simulation times. The key observation is that, while the existing formulations add a significant amount of diffusion almost everywhere, the proposed formulation automatically introduces numerical dissipation *only* in the neighborhood of the sharp features of the solution. The latter is precisely the desired behavior of a discontinuity-capturing mechanism.

Water-gas injection in a reservoir This second application involves simultaneous injection of water and gas into a porous medium that is initially filled with oil and gas (and a small amount of water), as shown in **Fig. 12**. Initially, the medium has constant normalized saturations:

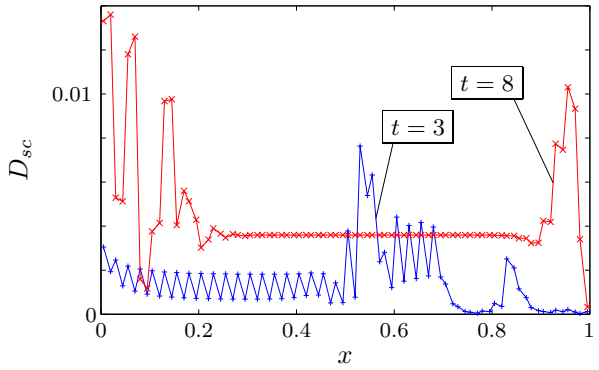

Fig. 10— Profiles of shock capturing diffusion introduced by the "canonical form" at two different times.

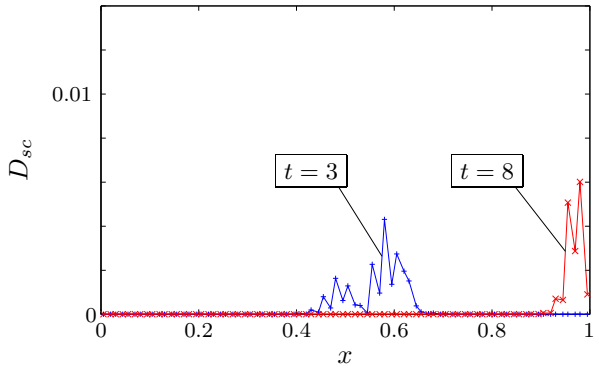

Fig. 11— Profiles of shock capturing diffusion introduced by the proposed formulation at two different times.

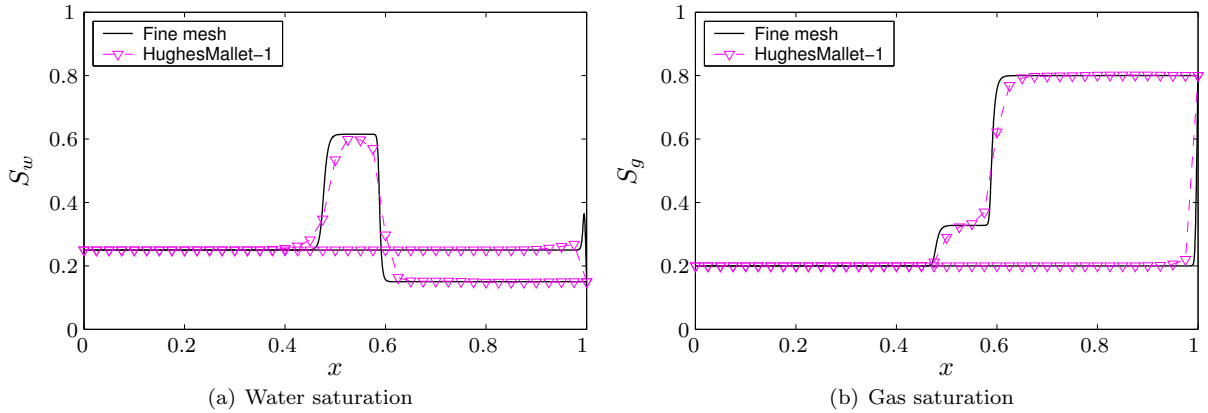

(a) Water saturation (b) Gas saturation

Fig. 8— Saturation profiles of the ASGS solution to the oil filtration problem. "Canonical form" of the shock-capturing diffusion.

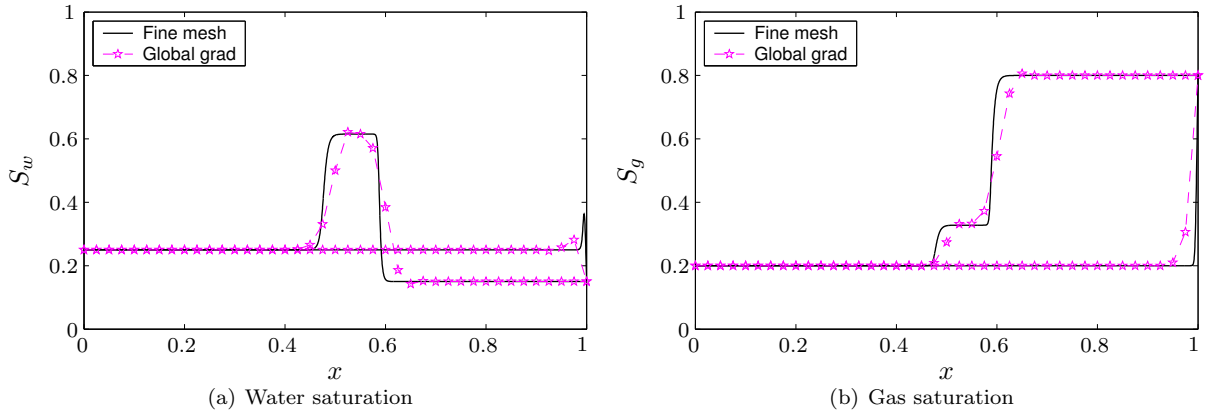

(a) Water saturation (b) Gas saturation

Fig. 9— Saturation profiles of the ASGS solution to the oil filtration problem. Proposed formulation of the shock-capturing diffusion.

$S_w = 0.05$, $S_g = 0.4$, and $S_o = 0.55$. Gas and water are injected in such proportion that the normalized water and gas saturations at the inlet are $S_w = 0.85$ and $S_g = 0.15$, respectively. The injected saturations are assumed to be constant throughout the experiment. The values of initial and injected saturations used in this example are representative of a linear water-alternating-gas (WAG) injection process in a hydrocarbon reservoir after primary production.[28, 29]

Analytical solution The analytical solution to the water-gas injection problem described above is a sequence of two waves, where the slow wave is a rarefaction-shock, and the fast wave is a single shock.[12] In **Fig. 13** we plot the analytical solution in saturation space. The solid line is the rarefaction curve —where the solution is continuous—, and the dashed lines are the shock curves, which correspond to discontinuities.

The fluid saturation profiles of the analytical solution to the water-gas injection problem are shown in **Fig. 14**. Because the capillarity-free solution is self-similar, the profiles are plotted against the similarity variable $\zeta = x/t$. The slow wave involves mainly displacement of oil by injected water, and the fast wave corresponds to a displacement of gas by oil. An oil bank with higher oil saturations than those of the initial and injected states is formed. This is characteristic of water flood processes in the presence of free gas.[30, 31]

"Reference" numerical solution We compute a "reference" numerical solution to the water-gas injection problem with small capillary diffusion coefficients:

$$\epsilon_w = 0.001, \quad \epsilon_g = 0.002. \tag{38}$$

We use the standard Galerkin formulation on a very fine mesh of 4000 elements ($h = 2.5 \times 10^{-4}$), and a Crank-Nicolson time integration scheme with $\delta t = 5 \times 10^{-5}$. For this space and time discretization, the element Peclet and Courant numbers are, respectively:

$$Pe := \frac{\sigma_{\max} h}{\epsilon_{\min}} \approx 0.3, \tag{39}$$

$$Co := \frac{\sigma_{\max} \delta t}{h} \approx 0.25. \tag{40}$$

In **Fig. 15** we plot the water and gas saturation profiles of the "reference" numerical solution at $t = 0.5$, together with the capillarity-free analytical solution. The numerical solution correctly captures the location and magnitude

Fig. 12— Sketch of the water-gas injection problem. Water and gas are injected into a medium initially filled with oil and gas.

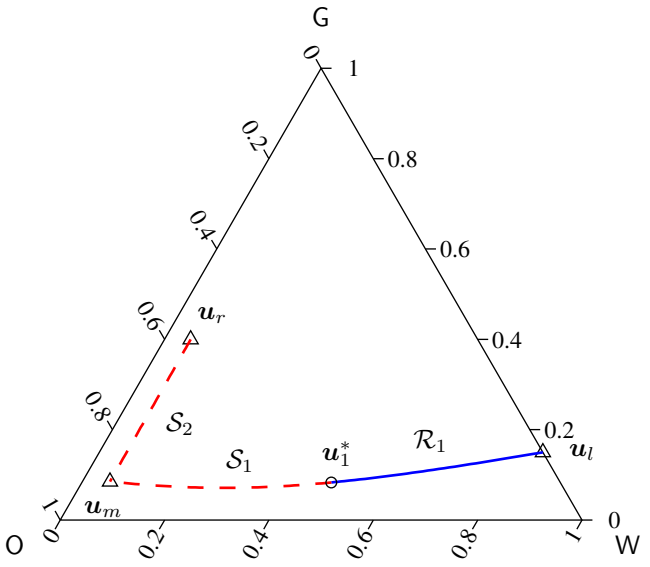

Fig. 13— Saturation path of the exact solution to the water-gas injection problem. The slow wave is a rarefaction-shock and the fast wave is a genuine shock.

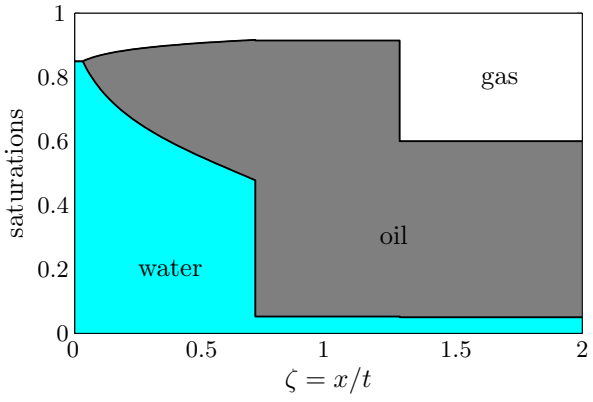

Fig. 14— Saturation profiles of the exact solution to the water-gas injection problem. Saturations of each phase are plotted against the similarity variable $\zeta = x/t$.

of the shocks, and provides an accurate representation of the rarefaction fan. As was the case in the oil filtration example, additional simulations with different space and time discretizations, and different capillary diffusion coefficients, confirm convergence of the standard Galerkin method to the entropy solution of the problem.

Standard Galerkin solution The water-gas injection problem is solved with the same physical parameters on a much coarser mesh of 40 elements and a time step $\delta t = 0.005$. The element Peclet number is now $Pe \approx 30$, and the element Courant number remains $Co \approx 0.25$. The results are shown in **Fig. 16** at two different simulation times ($t = 0.5$ and $t = 2$), and compared with the reference numerical solution. Clearly, the standard Galerkin solution on the coarse mesh is unstable. The Galerkin solution is completely oscillatory, especially after breakthrough of the water front.

Algebraic subgrid scale solutions The numerical solution produced by the ASGS method with the $\boldsymbol{\tau}$ formulation of Hughes and Mallet[24] is shown in **Fig. 17**. The behavior of the method is remarkable, considering that a very coarse mesh of only 40 elements was used. The stabilizing term is able to remove the global oscillatory behavior of the standard Galerkin method. The solution is also extremely accurate and preserves a sharp definition of the shocks and boundary layers.

It should be noted, however, that other formulations of the matrix $\boldsymbol{\tau}$ of stabilizing coefficients[25,32] do not yield the impressive results of Figure 17. In some cases they even fail to converge, emphasizing the importance of an appropriate choice of $\boldsymbol{\tau}$ for each particular problem.

Stabilized solutions with shock capturing diffusion Despite the effective stabilization of the ASGS method with the matrix of stabilizing coefficients given by Hughes and Mallet,[24] some local overshooting is still present in the solution (see Figure 17). We make use of a discontinuity-capturing technique to remove the spurious wiggles. In **Fig. 18** we plot the numerical solution obtained after using the ASGS method above in conjunction with the proposed "global-gradient form" of the shock-capturing diffusion —Eq. (29)— with the following parameters:

$$\boldsymbol{U}_{sc} = (0.5, 0.5), \qquad C_{sc} = 2. \tag{41}$$

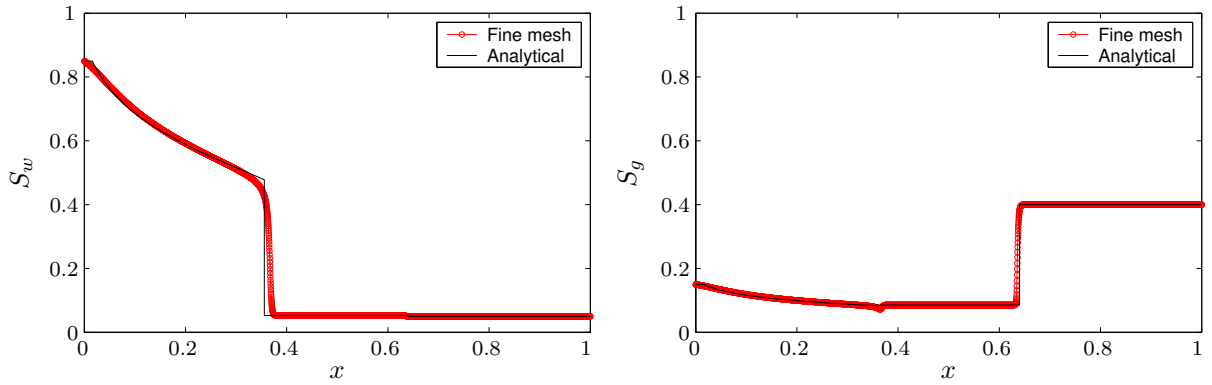

(a) Water saturation (b) Gas saturation

Fig. 15— Saturation profiles of the standard Galerkin solution to the water-gas injection problem on a fine mesh of 4000 elements, and comparison to the analytical solution of the capillarity-free case. Results are shown at time $t = 0.5$.

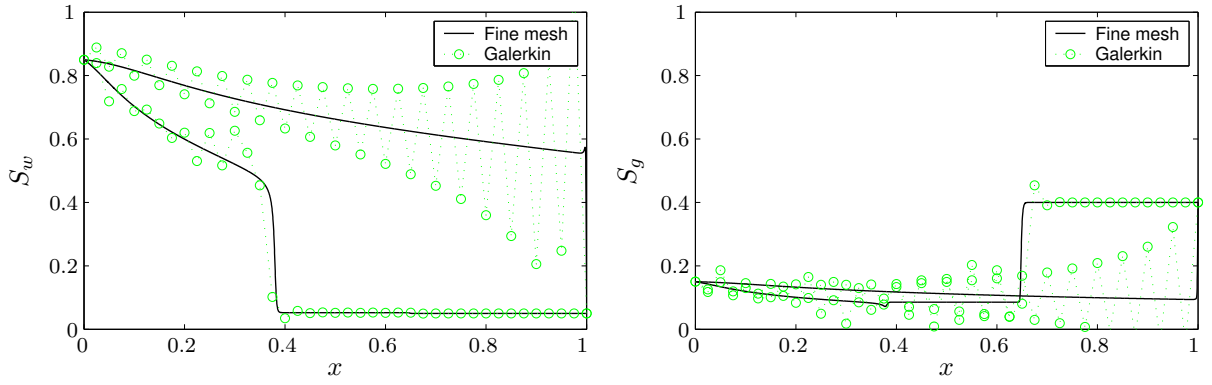

(a) Water saturation (b) Gas saturation

Fig. 16— Saturation profiles of the standard Galerkin solution to the water-gas injection problem on a coarse mesh of 40 elements. Results are shown at times $t = 0.5$ and $t = 2$.

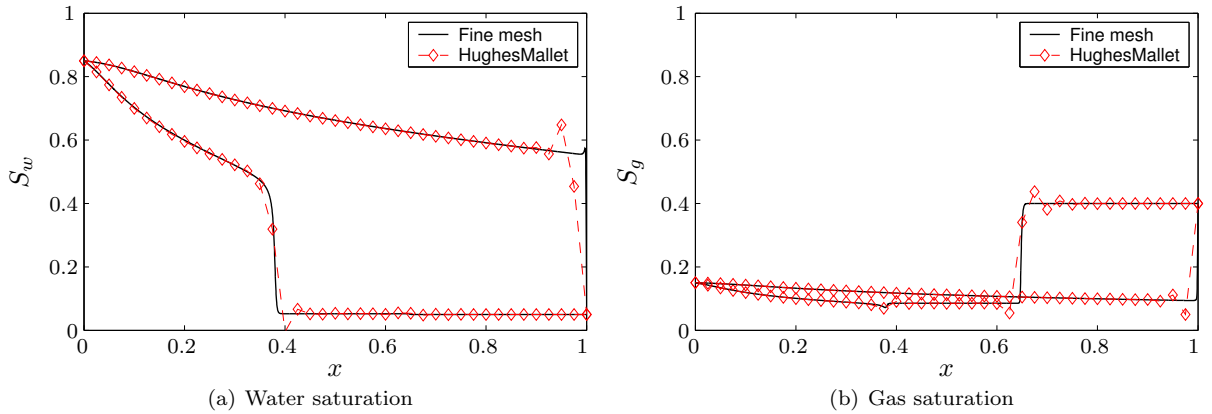

(a) Water saturation (b) Gas saturation

Fig. 17— Saturation profiles of the ASGS solution (τ formulation given by Hughes and Mallet[24]) to the water-gas injection problem on the coarse mesh.

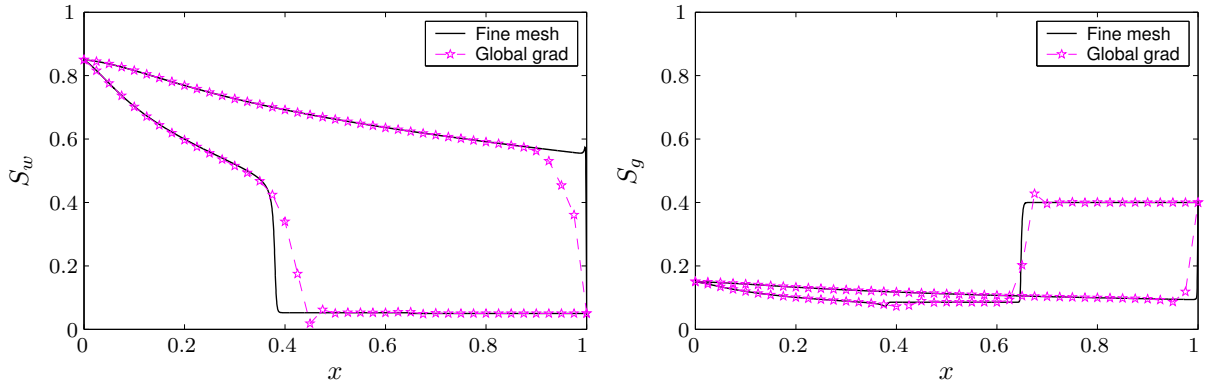

(a) Water saturation (b) Gas saturation

Fig. 18— Saturation profiles of the ASGS solution to the water-gas injection problem. Proposed formulation of shock-capturing diffusion.

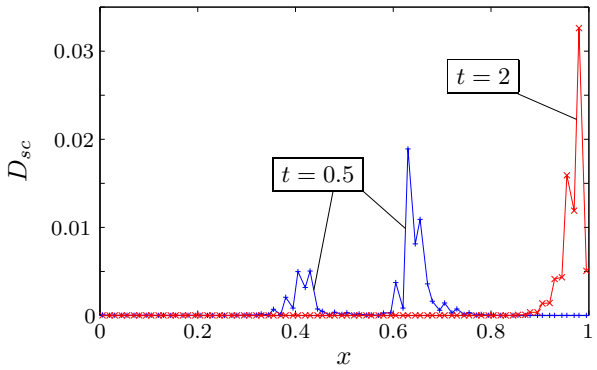

Fig. 19— Profiles of shock capturing diffusion introduced by the proposed formulation at two different times.

The computed solution retains exceptional accuracy in the smooth regions —the rarefaction fan and the constant saturation states— while effectively enhancing stability near the sharp gradients.

The profile of additional diffusion introduced by the discontinuity-capturing term is plotted —at simulation times $t = 0.5$ and $t = 2$— in **Fig. 19**. It is apparent that the amount of artificial diffusion is negligible everywhere, except: (1) in the vicinity of both shocks during transient conditions; (2) near the boundary layer for quasi-steady conditions. The "canonical form" of the shock-capturing diffusion described earlier is either less effective or even fails to converge.

Conclusions

We have presented a fairly general formulation for the numerical solution of nonlinear systems of conservation laws, and applied it to the equations of one-dimensional three-phase flow through porous media. The method is based on the original framework developed by Hughes,[3] and entails a multiple-scale decomposition of the solution into resolved and unresolved scales. It is precisely the effect of the unresolved subgrid scales on the resolved grid scales that introduces a stabilizing term in the formulation. Key distinctive features of the formulation developed herein are: (1) the multiscale split is performed *before* any linearization of the equations (which are kept in conservation form); (2) the multiscale solution is *not* reconstructed from point values of coarse-scale and subgrid-scale solutions; and (3) a novel shock-capturing technique is proposed to further enhance stability of the solution in the neighborhood of strong gradients.

From the results presented, we conclude that the proposed stabilized method yields numerical solutions of exceptional quality to challenging, highly nonlinear, nearly hyperbolic problems. Solutions computed on very coarse grids display excellent stability and accuracy. The algebraic subgrid model employed is quite sensitive, however, to the choice of the matrix of stabilizing coefficients $\boldsymbol{\tau}$. The definition of $\boldsymbol{\tau}$ given by Hughes and Mallet,[24] which requires the solution of an eigenvalue problem, seems to be the most applicable to the type of problems considered in this paper. This observation is further confirmed by numerical experiments with other one-dimensional systems that become strictly hyperbolic in the limit of vanishing diffusion —such as the shallow-water equations and the Euler equations of gas dynamics—.

The novel formulation of the discontinuity-capturing diffusion —coined "global-gradient form"— provides an alternative to existing formulations. The simulations clearly show that, in contrast to the canonical expressions, the numerical diffusion introduced by the proposed formulation is confined to the vicinity of discontinuities in the solution.

Several issues deserve further investigation. One of the topics that is currently being addressed is the study of a different approximation to the subscales. In particular, we are interested in a *numerical* approximation of the subgrid scale problem with appropriate basis functions —high-order finite elements, wavelets, *etc.*—, which are potentially capable of capturing the sharp features of the solution that the coarse mesh is unable to resolve.

Nomenclature

Roman letters

$\mathbf{D}$	capillary-diffusion tensor, L^2/t
D_{sc}	shock-capturing diffusion coefficient, L^2/t
$\boldsymbol{f}$	$=(f_w, f_g)$, vector of fractional flows, dimensionless
f_α	$=\lambda_\alpha/\lambda_T$, fractional flow of the α-phase, dimensionless
h	element size, L
k	absolute permeability, L^2
$k_{r\alpha}$	relative permeability of the α-phase, dimensionless
L	length of the one-dimensional domain, L
$\mathcal{L}^*_{u_h}$	adjoint of a linearized advection-diffusion operator, 1/t
n	outward unit normal to the boundary, dimensionless
p_α	pressure of the α-phase, $\mathrm{m/Lt}^2$
$P_{c\alpha}$	$=p_\alpha - p_o$, capillary pressure of the α-phase, $\mathrm{m/Lt}^2$
$P^D_{c\alpha}$	$=P_{c\alpha}/P^*_{c\alpha}$, dimensionless capillary pressure of the α-phase
$P^*_{c\alpha}$	$=\int_0^1 \lvert P_{c\alpha}(s)\rvert \,\mathrm{d}s$, characteristic capillary pressure of the α-phase
$\mathcal{R}(\boldsymbol{u}_h)$	grid scale residual, 1/t
S_α	saturation of the α-phase, dimensionless
t	time, t
t_D	$=(1/L)\int_0^t v_T(\tau)\,\mathrm{d}\tau$, dimensionless time
$\boldsymbol{u}$	$=(S_w, S_g)$, vector of saturations, dimensionless
$\boldsymbol{u}_h$	coarse scale solution, dimensionless
$\tilde{\boldsymbol{u}}$	subgrid scale solution, dimensionless
$\boldsymbol{v}$	test function, dimensionless
v_α	$=-\frac{k}{\phi}\frac{k_{r\alpha}}{\mu_\alpha}\partial_x p_\alpha$, velocity of the α-phase, L/t
v_T	$=\sum_\alpha v_\alpha$, total velocity, L/t
x	space coordinate, L
x_D	$=x/L$, dimensionless space coordinate

Greek letters

Γ_u	boundary with essential boundary conditions
Γ_n	boundary with natural boundary conditions
δt	time step, t
ϵ_α	$=\frac{(k/\phi)}{v_T L}P^*_{c\alpha}$, capillary diffusion coefficient of the α-phase, L^2/t
ζ	$=x/t$, self-similarity variable, L/t
λ_T	$=\sum_\alpha \lambda_\alpha$, total mobility, Lt/m
λ_α	relative mobility of the α-phase, Lt/m
μ_α	dynamic viscosity of the α-phase, m/Lt
$\boldsymbol{\tau}_h$	matrix of intrinsic time scales, t
ϕ	porosity, dimensionless
Ω	one-dimensional spatial domain, L

Subscripts

g	gas phase
o	oil phase
w	water phase
l	left state
r	right state

Acknowledgements

This work was supported in part by the U.S. Department of Energy under Contract No. DE-AC03-76SF00098.

References

[1] G. Chavent and J. Jaffré. *Mathematical Models and Finite Elements for Reservoir Simulation*, volume 17 of *Studies in Mathematics and its Applications*. Elsevier, North-Holland, 1986.

[2] L. P. Franca (ed.). Special issue on "Advances in stabilized methods in computational mechanics". *Comput. Methods Appl. Mech. Engrg.*, 166(1–2), 1998.

[3] T. J. R. Hughes. Multiscale phenomena: Green's functions, the Dirichlet-to-Neumann formulation, subgrid scale models, bubbles and the origins of stabilized methods. *Comput. Methods Appl. Mech. Engrg.*, 127:387–401, 1995.

[4] T. J. R. Hughes, G. R. Feijóo, L. Mazzei, and J.-B. Quincy. The variational multiscale method—a paradigm for computational mechanics. *Comput. Methods Appl. Mech. Engrg.*, 166:3–24, 1998.

[5] R. Juanes and T. W. Patzek. Multiple scale stabilized finite elements for the simulation of tracer injections and waterflood. In *SPE/DOE Thirteenth Symposium on Improved Oil Recovery*, Tulsa, OK, April 13–17, 2002. (SPE 75231). Submitted to *Soc. Pet. Eng. J.*

[6] R. Juanes and T. W. Patzek. Multiscale-stabilized finite element methods for miscible and immiscible flow in porous media. *J. Hydraul. Res.*, 2002. (Accepted, In Press). Also available as Report LBNL-50382, Lawrence Berkeley National Laboratory.

[7] T. Y. Hou and X.-H. Wu. A multiscale finite element method for elliptic problems in composite materials and porous media. *J. Comput. Phys.*, 134:169–189, 1997.

[8] T. Arbogast. Numerical subgrid upscaling of two-phase flow in porous media. In Z. Chen, R. E. Ewing, and Z.-C. Shi, editors, *Numerical Treatment of Multiphase Flow in Porous Media*, volume 552 of *Lecture Notes in Physics*, pages 35–49, Berlin, 2000. Springer.

[9] T. Arbogast. Implementation of a locally conservative numerical subgrid upscaling scheme for two-phase Darcy flow. *Comput. Geosci.*, 6(3–4):453–481, 2002.

[10] M. Peszynska, M. F. Wheeler, and I. Yotov. Mortar upscaling for multiphase flow in porous media. *Comput. Geosci.*, 6(1):73–100, 2002.

[11] A. Masud and T. J. R. Hughes. A stabilized mixed finite element method for Darcy flow. *Comput. Methods Appl. Mech. Engrg.*, 191(39–40):4341–4370, 2002.

[12] R. Juanes and T. W. Patzek. Analytical solution to the Riemann problem of three-phase flow in porous media. *Transp. Porous Media*, 2002. (Accepted). Also available as Report LBNL-51552, Lawrence Berkeley National Laboratory.

[13] R. E. Guzmán. *Mathematics of Three-Phase Flow*. PhD Dissertation, Stanford University, July 1995.

[14] R. Juanes. *Displacement theory and multiscale numerical modeling of three-phase flow in porous media*. PhD Dissertation, University of California at Berkeley, March 2003.

[15] R. Juanes and T. W. Patzek. Relative permeabilities for strictly hyperbolic models of three-phase flow in porous media. *Transp. Porous Media*, 2002. (Submitted). Also available as Report LBNL-51442, Lawrence Berkeley National Laboratory.

[16] R. Juanes and T. W. Patzek. Strictly hyperbolic models of co-current three-phase flow with gravity. *Transp. Porous Media*, 2002. (Submitted). Also available as Report LBNL-51845, Lawrence Berkeley National Laboratory.

[17] H. L. Stone. Probability model for estimating three-phase relative permeability. *J. Pet. Technol.*, 23(2):214–218, February 1970. *Petrol. Trans.* AIME, 249.

[18] H. L. Stone. Estimation of three-phase relative permeability and residual oil data. *J. Can. Petrol. Technol.*, 12(4):53–61, 1973.

[19] R. Lenormand. Pattern growth and fluid displacements through porous media. *Physica A*, 140:114–123, 1986.

[20] M. C. Leverett and W. B. Lewis. Steady flow of gas-oil-water mixtures through unconsolidated sands. *Petrol. Trans.* AIME, 142:107–116, 1941.

[21] K. Aziz and A. Settari. *Petroleum Reservoir Simulation*. Elsevier, London, 1979.

[22] R. Juanes and T. W. Patzek. Three-phase displacement theory: An improved description of relative permeabilities. In *SPE Annual Technical Conference and Exhibition*, San Antonio, TX, September 29–October 2, 2002. (SPE 77539). Submitted to *Soc. Pet. Eng. J.*

[23] R. Codina and J. Blasco. Analysis of a stabilized finite element approximation of the transient convection-diffusion-reaction equation using orthogonal subscales. *Comput. Visual. Sci.*, 4(3):167–174, 2002.

[24] T. J. R. Hughes and M. Mallet. A new finite element formulation for computational fluid dynamics: III. The generalized streamline operator for multidimensional advective-diffusive systems. *Comput. Methods Appl. Mech. Engrg.*, 58:305–328, 1986.

[25] R. Codina. On stabilized finite element methods for linear systems of convection-diffusion-reaction equations. *Comput. Methods Appl. Mech. Engrg.*, 188:61–82, 2000.

[26] R. Codina. A discontinuity-capturing crosswind-dissipation for the finite element solution of the convection-diffusion equation. *Comput. Methods Appl. Mech. Engrg.*, 110:325–342, 1993.

[27] R. Juanes and T. W. Patzek. Relative permeabilities in co-current three-phase displacements with gravity. In *SPE Western Regional/AAPG Pacific Section Joint Meeting*, Long Beach, CA, May 19–24 2003. (SPE 83445). Submitted to *Soc. Pet. Eng. J.*

[28] J. R. Christensen, E. H. Stenby, and A. Skauge. Review of WAG field experience. *SPE Reserv. Eng.*, 4(2):97–106, April 2001.

[29] D. Marchesin and B. J. Plohr. Wave structure in WAG recovery. *Soc. Pet. Eng. J.*, 6(2):209–219, June 2001.

[30] J. R. Kyte, R. J. Stanclift Jr., S. C. Stephan Jr., and L. A. Rapoport. Mechanism of water flooding in the presence of free gas. *Petrol. Trans.* AIME, 207:215–221, 1956.

[31] G. P. Willhite. *Waterflooding*, volume 3 of *SPE Textbook Series*. Society of Petroleum Engineers, Richardson, TX, 1986.

[32] F. Shakib, T. J. R. Hughes, and Z. Johan. A new finite element formulation for computational fluid dynamics: X. The compressible Euler and Navier-Stokes equations. *Comput. Methods Appl. Mech. Engrg.*, 89:141–219, 1991.